Spectrochimica Acta Part A 82 (2011) 414–423

Contents lists available at ScienceDirect

Spectrochimica Acta Part A: Molecular and Biomolecular Spectroscopy

journal homepage: www.elsevier.com/locate/saa

Synthesis, structural characterization and antimicrobial activity evaluation of metal complexes of sparfloxacin

Nadia E.A. El-Gamel*, M.A. Zayed

Chemistry Department, Faculty of Science, Cairo University, Gamma Street 12613, Giza, Egypt

ARTICLE INFO

Article history:
Received 4 June 2011
Received in revised form 17 July 2011
Accepted 20 July 2011

Keywords:
Sparfloxacin (**HL$_1$**)
DL-Alanine (**H$_2$L$_2$**)
Binary and ternary complexes
Spectral studies
Thermal analysis
Antimicrobial activity

ABSTRACT

The synthesis and characterization of binary Cu(II)- (**1**), Co(II)- (**2**), Ni(II)- (**3**), Mn(II)- (**4**), Cr(III)- (**5**), Fe(III)- (**6**), La(III)- (**7**), UO_2(VI)- (**8**) complexes with sparfloxacin (**HL$_1$**) and ternary Cu(II)- (**9**), Co(II)- (**10**), Ni(II)- (**11**), Mn(II)- (**12**), Cr(III)- (**13**), Fe(III)- (**14**), La(III)- (**15**), UO_2(VI)- (**16**) complexes with sparfloxacin (**HL$_1$**) and DL-alanine (**H$_2$L$_2$**) complexes are reported using elemental analysis, molar conductance, magnetic susceptibility, IR, UV–Vis, thermal analysis and ^{1}H-NMR spectral studies.

The molar conductance measurements of all the complexes in DMF solution correspond to non-electrolytic nature.

All complexes were of the high-spin type and found to have six-coordinate octahedral geometry except the Cu(II) complexes which were four coordinate, square planar and U- and La-atoms in the uranyl and lanthanide have a pentagonal bipyramidal coordination sphere. The antimicrobial activity of these complexes has been screened against two Gram-positive and two Gram-negative bacteria. Antifungal activity against two different fungi has been evaluated and compared with reference drug sparfloxacin. All the binary and ternary complexes showed remarkable potential antimicrobial activity higher than the recommended standard agents. Ni(II)- and Mn(II) complexes exhibited higher potency as compared to the parent drug against Gram-negative bacteria.

1. Introduction

The development of metal complexes as artificial nucleases is an area of interest. Floroquinolone derivatives possess a broad spectrum of activity against various pathogenic microorganisms, which are resistant to aminoglycosides, penicillins, cephalosporins, tetracyclines and other antibiotics. This class of compounds, when compared to existing bactericidal drugs, shows improved pharmacokinetic properties and a broad spectrum of activity against parasites, bacteria, and mycobacteria, including resistant strains; in addition to that they displayed significant in vitro antibacterial activity against many Gram-positive and Gram-negative bacteria through inhibition of their DNA gyrase [1].

Sparfloxacin (**HL$_1$**, 5-amino-1-cyclopropyl-7-(3,5-dimethyl-1-piperazinyl)-6,8-difluoro-1,4-dihydro-4-oxo-3-quinoline-carboxylic acid) (Fig. 1) is widely used in the treatment of urinary tract infections and is reported to exhibit higher activity against the major respiratory pathogens and typical pathogens that cause pneumonia [2].

Metal coordination to biologically active molecules can be used in order to enhance their biological activity; therefore, numerous studies regarding the interaction between quinolones with several metallic cations have reported in the literature. Some of these metal complexes represented potential antibacterial activity [3], for example Co(II) and Cu(II) complexes with sparfloxacin exhibited a significant enhancement against several pathogenic bacteria than sparfloxacin [4].

The antibacterial and antifungal properties of palladium and platinum complexes with sparfloxacin have also been reported, where the complexes showed activity against *Mycobacterium tuberculosis* strain [5].

Fluoroquinolones behaved as bidentate ligands binding to the metallic ion through the carboxylate and carbonyl oxygens as observed in case of complexes with metal ions such as Co(II), Ni(II), Zn(II), Cd(II), Mn(II) and Cu(II) [6]. Nevertheless, it was mentioned that the platinum complexes were chelated with fluoroquinolones via piperazine nitrogen atoms which is much less common [5a]. Recently some transition and earth metal complexes of sparfloxacin were prepared and characterized and the antifungal activity were evaluated where Fe(II), and Cd(II) complexes showed remarkable activity [7].

In this context, the present work describes the synthesis of binary and ternary complexes of sparfloxacin with DL-alanine

* Corresponding author. Tel.: +20 20112363028.
E-mail address: nadinealy@hotmail.com (N.E.A. El-Gamel).

1386-1425/$ – see front matter © 2011 Elsevier B.V. All rights reserved.
doi:10.1016/j.saa.2011.07.072

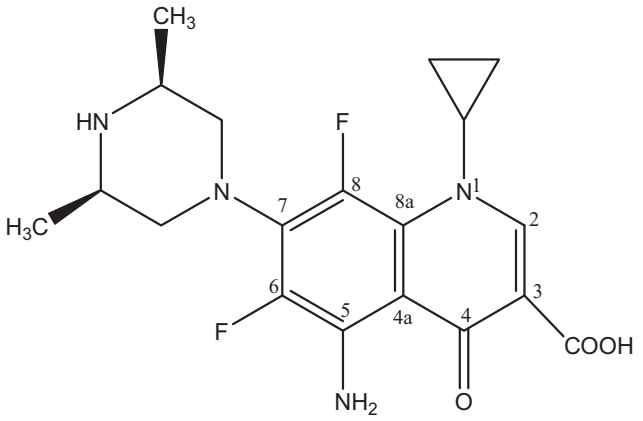

Fig. 1. The structure of sparfloxacin (**HL_1**).

with various metal ions like Cu(II), Co(II), Ni(II), Mn(II), Cr(III), Fe(III), La(III) and UO_2(VI), in order to continue the exploration of the coordination behavior adopted by fluoroquinolones. For the characterization of the compounds the following spectroscopic and analytical techniques were employed: elemental analyses, IR and ^{1}H-NMR spectroscopy, UV–Vis, solid reflectance, magnetic moment, ESR and thermogravimetric analysis. The biological activity of the parent ligand and its metal complexes is evaluated where high antimicrobial is recorded.

2. Experimental

2.1. Materials and reagents

All chemicals used were of the analytical reagent grade (AR) and of highest purity available. They included sparfloxacin, DL-alanine, $Cu(II)Cl_2{\cdot}2H_2O$, $La(NO_3)_3{\cdot}6H_2O$, $UO_2(NO_3)_2{\cdot}6H_2O$, and $MnCl_2$ (Sigma), $Co(II)Cl_2{\cdot}6H_2O$, $CrCl_3{\cdot}6H_2O$ and $Ni(II)Cl_2{\cdot}6H_2O$ (BDH); $FeCl_3{\cdot}6H_2O$ (Prolabo) were used. Absolute ethyl alcohol, diethyl ether (Adwic), yeast extract and agar (Sigma) were also used. De-ionized water collected from all glass equipments was usually used in all preparations.

2.2. Instruments

FTIR spectra were obtained from dispersions in KBr using a Perkin-Elmer FT-IR type 1650 spectrophotometer. The spectra were collected in the range from 200 to 4000 cm^{-1} with a resolution of 2 cm^{-1}. UV–Vis spectrophotometric measurements were carried out using automated spectrophotometer UV-Vis Thermo Fischer Scientific Model Evolution 60 ranged from 200 to 900 nm. The molar magnetic susceptibility was measured on powdered samples using the Faraday method. The diamagnetic corrections were made by Pascal's constant and $Hg[Co(SCN)_4]$ was used as a calibrant. The solid reflectance spectra were performed on a Shimadzu 3101pc spectrophotometer. The ESR spectra were recorded on JES FA-300 spectrophotometer at room temperature. Molar conductance was measured on a ELICO(CM82T) conductivity bridge. ^{1}H-NMR spectra were recorded on a BRUKER DPX 400 instrument at room temperature (d_6-DMSO solution with TMS as internal standard). Thermal analyses of the complexes were carried out using a Shimadzu TGA-50H and DTA-50H thermogravimetric analyzer in a dynamic nitrogen atmosphere (flow rate 20 ml min^{-1}) with a heating rate of 10 °C min^{-1}. The percentage weight loss was measured from ambient temperature to 1000 °C. Highly sintered α-Al_2O_3 was used as reference.

2.3. Antimicrobial activity

Antimicrobial activity of the tested samples was determined using a modified Kirby-Bauer disc diffusion method [8]. 100 μl of the test bacteria/fungi were grown in 10 ml of fresh media until they reached a count of approximately 108 cells/ml for bacteria or 105 cells/ml for fungi [9]. 100 μl of microbial suspension was spread onto agar plates. Plates inoculated with filamentous fungi as *Aspergillus flavus*, *Candida albicans* at 25 °C for 48 h; Gram (+) bacteria as *Staphylococcus aureus*; Gram (−) bacteria as *Escherichia coli*; they were incubated at 35–37 °C for 24–48 h and yeast as *C. albicans* incubated at 30 °C for 24–48 h and, then the diameters of the inhibition zones were measured in millimeters [9]. Standard discs of **Tetracycline** (antibacterial agent), **Amphotericin B** (antifungal agent) served as positive controls, while filter discs impregnated with 10 μl of solvent (distilled water, chloroform, DMSO) were used as a negative control.

2.4. Synthesis of the complexes

Metal complexes were synthesized by addition of a hot water–ethanolic solution (60 °C) of the metal chlorides for Cu(II), Co(II) Ni(II), Mn(II), Cr(III) and Fe(III), nitrate for UO_2(VI) and La(III) (25 ml, 0.1 mmol) to a hot ethanolic solution of **HL_1** (25 ml, 0.2 mmol in case of binary or 0.1 mmol in case of ternary complexes) and DL-alanine (0.1 mmol). The resulting mixture was stirred under reflux for 2 h and left to cool, whereby the complexes precipitated as fine powders. The solid complexes were filtered, washed with ethanol, then with diethyl ether, and dried in a vacuum desiccator over anhydrous calcium chloride.

3. Results and discussion

The found and calculated percentages of elemental analysis (CHN) data are in well agreement with each other and prove the suggested molecular formulas of the complexes (Tables 1 and 2). The molar conductance measurements of all the complexes in DMF solution were in the range of 18.10–11.99 Ω^2 cm^{-1} mol^{-1}. These relatively low values indicate non-electrolytic nature of the complexes [10].

3.1. IR spectral studies

All the characteristic absorption bands of the complexes are represented in Table 3. The pyridone stretch $\nu(C{=}O)_p$ in **HL_1** appears at 1641 cm^{-1} and the asymmetric and symmetric stretching $\nu(COO)_{carb}$ appeared at 1716 and 1371 cm^{-1}, respectively. The pyridone band is shifted to lower frequency (3–9 cm^{-1}) and (3–11 cm^{-1}) in binary and ternary complexes, which indicates the involvement in the chelation [3a]. The participation of the carboxylate O atom in the binary and ternary complexes is confirmed by low shift in position of these bands to (1613–1555 cm^{-1}) and high shift to (1400–1380 cm^{-1}) for asymmetric and symmetric bands, respectively [3a].

IR spectrum of **H_2L_2** shows sharp bands at 1594 and 1410 cm^{-1} assigned to the asymmetric and symmetric stretching vibrations of the carboxylate moiety, respectively. These bands are shifted to lower (3–63 cm^{-1}) or higher (6–22 cm^{-1}) frequencies, indicating that **H_2L_2** coordinates to the metal ions via deprotonated carboxylate [11].

The IR spectra of all complexes exhibit a broad split band between 3400 and 3150 cm^{-1} which the N–H stretching vibration of the piperazinyl moiety [12,13], therefore it is quite difficult to detect the coordination vibration band of NH_2 of **H_2L_2**; therefore we focused on in-plane bending, (NH_2) vibration and the shift of this band from 1521 cm^{-1} to 1502–1517 cm^{-1} indicates participation in

Table 1
Analytical and physical data of binary metal complexes.

Compound	Color (% yield)	m.p (°C)	Found (calculated) (%)			μ_{eff} (B.M.)	Λ_m (Ω^2 mol^{-1} cm^{-1})
			C	H	N		
Sparfloxacin (**HL$_1$**)	Yellow	240	57.95	5.55	14.20	–	–
$C_{19}H_{22}F_2N_4O_3$			(58.16)	(5.65)	(14.28)		
[Cu(II)(L$_1$)$_2$]·2H$_2$O	Green	290	51.50	5.45	12.53	1.74	18.10
$C_{38}H_{46}CuF_4N_4O_8$	(75)		(51.73)	(5.25)	(12.70)		
[Co(II)(L$_1$)$_2$·2H$_2$O]	Olive green	>300	52.16	5.92	12.03	4.9	15.26
$C_{38}H_{46}CoF_4N_8O_8$	(85)		(52.00)	(5.28)	(12.77)		
[Ni(II)(L$_1$)$_2$·2H$_2$O]	Yellowish green	>300	52.41	5.22	12.63	3.23	12.29
$C_{38}H_{46}F_4N_8NiO_8$	(75)		(52.01)	(5.28)	(12.77)		
[Mn(II)(L$_1$)$_2$·2H$_2$O]	Mustard	286	51.94	5.59	12.55	5.73	14.25
$C_{38}H_{46}F_4MnN_8O_8$	(88)		(52.24)	(5.31)	(12.82)		
[Cr(III)(L$_1$)$_2$Cl·H$_2$O]·H$_2$O	Dark green	>300	50.00	5.10	12.42	3.87	13.95
$C_{38}H_{46}ClCrF_4N_8O_8$	(85)		(50.36)	(5.12)	(12.36)		
[La(III)(L$_1$)$_2$·NO$_3$·H$_2$O]·2H$_2$O	Golden yellow	270	43.35	4.55	12.69	Diamagnetic	13.32
$C_{38}H_{48}F_4LaN_9O_{12}$	(87)		(43.98)	(4.66)	(12.15)		
[Fe(III)(L$_1$)$_2$·Cl·H$_2$O]·H$_2$O	Brown	289	50.32	5.20	12.02	5.90	17.24
$C_{38}H_{46}ClF_4FeN_8O_8$	(72)		(50.15)	(5.09)	(12.31)		
[UO$_2$(VI)(L$_1$)$_2$·H$_2$O]	Orange	279	42.50	4.20	10.02	Diamagnetic	15.14
$C_{38}H_{44}F_4N_8O_9U_1$	(65)		(42.62)	(4.14)	(10.46)		

Table 2
Analytical and physical data of ternary metal complexes.

Compound	Color (% yield)	m.p (°C)	Found (calculated) (%)			μ_{eff} (B.M.)	Λ_m (Ω^2 mol^{-1} cm^{-1})
			C	H	N		
[Cu(II)(L$_1$)(HL$_2$)]·2H$_2$O	Green	>300	45.95	5.25	12.12	1.81	–
$C_{22}H_{31}CuF_2N_5O_7$			(45.63)	(5.40)	(12.09)		
[Co(II)(L$_1$)(HL$_2$)·2H$_2$O]	Green	290	46.23	5.45	12.53	5.10	17.66
$C_{22}H_{31}CoF_2N_5O_7$	(75)		(46.00)	(5.44)	(12.19)		
[Ni(II)(L$_1$)(HL$_2$)·2H$_2$O]	Light green	>300	46.16	5.42	12.03	3.36	16.94
$C_{22}H_{31}F_2N_5NiO_7$	(65)		(46.02)	(5.44)	(12.20)		
[Mn(II)(L$_1$)(HL$_2$)·2H$_2$O]	Mustard yellow	>300	46.41	5.28	12.63	5.41	11.99
$C_{22}H_{31}F_2MnN_5O_7$	(78)		(46.32)	(5.48)	(12.28)		
[Cr(III)(L$_1$)(HL$_2$)Cl·H$_2$O]·H$_2$O	Dark green	>300	42.94	5.29	11.55	3.85	14.95
$C_{22}H_{31}ClCrF_2N_5O_7$	(85)		(43.82)	(5.18)	(11.62)		
[La(III)(L$_1$)(HL$_2$)·NO$_3$·H$_2$O]·H$_2$O	Dark yellow	>300	36.00	4.19	11.42	Diamagnetic	13.95
$C_{22}H_{31}F_2LaN_6O_{10}$	(95)		(36.88)	(4.36)	(11.73)		
[Fe(III)(L$_1$)(HL$_2$)Cl·H$_2$O]·H$_2$O	Reddish brown	>300	43.35	5.55	11.69	5.92	17.78
$C_{22}H_{31}ClF_2FeN_5O_7$	(89)		(43.55)	(5.15)	(11.54)		
[UO$_2$(VI)(L$_1$)(HL$_2$)·H$_2$O]	Orange	>300	43.64	3.29	10.52	Diamagnetic	15.24
$C_{22}H_{29}F_2N_6O_7U_1$	(87)		(43.52)	(3.82)	(10.98)		

complex formation [14]. New bands in the complexes at 599–571 and 560–518 cm^{-1} can be assigned to the (M–O) stretching vibrations of the pyridone and carboxylate groups, respectively [14]. In ternary complexes bands in the 543–524 cm^{-1} and 430–415 cm^{-1} regions are attributed to the (M–O)$_{carb}$ and (M–N)$_{amino}$ stretching vibration of the carboxylate and amino groups [14]. There is a paucity of such assignments in the literature concerning lanthanide complexes, new band at 620 cm^{-1} and the new shoulder at 524 cm^{-1} and 361 cm^{-1} can be due to the La–O, La–N interactions, respectively [15]. Several bands are observed which are at

Table 3
IR spectral data (4000–400 cm^{-1}) of binary and ternary complexes.

Compound	ν(C=O)$_p$	ν(COO) (asym)	ν(COO) (sym.)	σNH$_2$	ν(COO) amino (sym.)	ν(COO) amino (asym)	ν(M–O)$_{carb}$	ν(M–O)$_p$	ν(M–O)$_{carb}$	ν(M–N)
HL$_1$	1641	1716	1371	–	–	–	–	–	–	–
1	1632	1555	1384	–	–	–	529	587	–	–
2	1638	1609	1384	–	–	––	525	597	–	–
3	1635	1612	1384	–	–	–	526	598	–	–
4	1634	1613	1390	–	–	–	528	588	–	–
5	1634	1611	1384	–	–	–	523	593	–	–
6	1636	1610	1385	–	–	–	528	571	–	–
7	1638	1608	1388	–	–	–	525	580	–	–
8	1638	1611	1385	–	––	–	518	586	–	–
9	1634	1612	1400	1515	1578	1419	520	588	540	420
10	1635	1611	1387	1517	1580	1420	520	592	530	425
11	1632	1606	1387	1509	1575	1419	540	599	534	419
12	1633	1607	1383	1508	1555	1408	533	590	532	415
13	1633	1608	1389	1505	1560	1418	530	585	543	418
14	1630	1607	1383	1508	1540	1402	533	590	548	418
15	1638	1610	1380	1512	1583	1512	520	588	524, 620	426
16	1636	1610	1383	1502	1583	1422	528	589	543	430

1105, 1490 and 1300 cm^{-1} can be assigned for symmetric bending, symmetric and asymmetric stretching of bidentate nitrate anions, which confirm that the NO_3 anion is used as bi-dentate in lanthanide complexes [16].

In uranyl chelates two intense sharp bands (920, 917 cm^{-1}); (775, 776 cm^{-1}) were reliably assigned to asymmetric and symmetric stretching vibrations of O=U=O in binary and ternary chelates, respectively [17]. In Cr(III) and Fe(III) complexes, medium bands below 300 cm^{-1} are observed due to ν(MCl) vibrations and further substantiate the mode of coordination as suggested by NMR spectral studies.

3.2. Electron spin resonance spectra

The ESR spectra for copper complex at room temperature gave the corresponding parameters of spin-Hamiltonian ($g\perp = 2.090$, 2.071; $g11 = 2.406$, 2.342) for binary and ternary complexes; respectively. This trend, $g11 > g\perp$ observed for the copper complexes suggests that the unpaired electron lies in the $d_{x^2-y^2}$ orbitals giving $^2B_{1g}$ as the ground state with $g11 > g\perp > 2$; the ESR parameters of the complexes coincide well with related systems which suggest that the complexes have square-planar geometry and the system is axially symmetric [18]. According to Hathaway [19] $G = gII - 2/g\perp - 2$; if the value of G is larger than four, exchange interaction is negligible because the local tetragonal axes are misaligned. The g values are 4.5 and 4.8 for the binary and ternary complexes, respectively, which suggests that the local tetragonal axis is aligned parallel or slightly misaligned and consistent with $d_{x^2-y^2}$ ground state.

3.3. Magnetic susceptibility and electronic spectra measurements

The magnetic moment values are calculated and reported in Tables 1 and 2. Cu(II) complexes have μ_{eff} values of 1.94 and 1.92 B.M., for **1** and **9**, respectively, indicating a square planar geometry; this was confirmed by the presence of one band in the spectrum at 13.385 cm^{-1} with two shoulders on either side at 18.860 and 11.900 cm^{-1}. These are assigned to $^2B_{1g} \rightarrow {}^2A_{1g}$, $^2B_{1g} \rightarrow {}^2B_{2g}$ and $^2B_{1g} \rightarrow {}^2E_{2g}$ transitions, respectively [20]. Cobalt(II) complexes have values of 4.9 and 5.1 B.M. for **2** and **10**, respectively, which indicate a high-spin octahedral configuration [17,21]. These complexes displaced three bands at 15.690–15.365, 17,467–18.019 and 21,930–22.120 cm^{-1} assigned to $^4T_{1g}(F) \rightarrow {}^4T_{2g}(F)(\nu_1)$, $^4T_{1g}(F) \rightarrow {}^4A_{2g}(F)(\nu_2)$ and $^4T_{1g}(F) \rightarrow {}^4T_{2g}(P)(\nu_3)$ transitions, respectively, confirming the octahedral geometry. Bands at 24.580–24.650 cm^{-1} could be attributed to charge transfer bands [22]. Nickel(II) complexes have a magnetic momentum of 3.23 and 3.36 B.M. for **3** and **11**, respectively indicating a high spin octahedral configuration [17,21]. The electronic spectra give three bands at $\nu_1 = 16.095$ cm^{-1}, $\nu_2 = 18.219$ cm^{-1} and $\nu_3 = 21.410$ cm^{-1}; these bands are assigned to $^3A_{2g} \rightarrow {}^3T_{2g}$, $^3A_{2g}(F) \rightarrow {}^3T_{1g}(F)$ and $^4A_{2g} \rightarrow {}^3T_{1g}(P)$ transitions, respectively. Bands at 24.550–24.680 cm^{-1} were observed, which could be attributed to LMCT [22]. Mn(II) complexes have μ_{eff} values of 5.73 and 5.84 B.M., for **4** and **12**, respectively indicating a high spin octahedral [22]. The electronic spectra of Mn(II) complexes show adsorption bands in the range (16,940–19,530 cm^{-1}), (22,218–24,268 cm^{-1}) and (26,310–27,765 cm^{-1}). These adsorption bands are assigned to $^6A_{1g} \rightarrow {}^4T_{1g}(^4G)$, $^6A_{1g} \rightarrow {}^4T_{2g}(^4G)$ and $^6A_{1g} \rightarrow {}^4E_g$, $^4A_{1g}(4G)$ transitions, respectively. These bands suggest the Mn(II) complexes posses an octahedral geometry [22]. μ_{eff} values for Cr(III) complexes have been reported to be 3.87 and 3.85 for **5** and **13**, respectively, this is in accordance to high spin octahedral geometry [22,23]. The solid reflectance spectra of Cr(III) complexes exhibited absorption bands in the range (13,260–19,415 cm^{-1}), (24,930–27,390 cm^{-1}) and 37,035–38,025 cm^{-1} due to $^4A_{2g}(F) \rightarrow {}^4T_{2g}(F)$, $^4A_{2g}(F) \rightarrow {}^4T_{1g}(F)$ and $^4A_{2g}(F) \rightarrow {}^4T_{1g}(P)$ d–d transitions, respectively. These bands suggest an octahedral geometry for the Cr(III) complexes [22]. Iron(III) complexes showed magnetic moment 5.90 and 5.92 B.M. for **6** and **14**, respectively corresponding to high spin octahedral geometry [17]. The reflectance spectra exhibited a band at the range of 21,295–20.904 cm^{-1}, assigned to the $^6A_{1g} \rightarrow {}^6T_{2g}(G)$ transition in octahedral geometry of the complex [36]. The $^6A_{1g} \rightarrow {}^6T_{1g}$ transition split into two bands at the range of 17,543–18.201 cm^{-1} and 14,995–12.141 cm^{-1}. These data are consistent with octahedral geometry [22]. The spectra showed bands at the range of 30.665–31.680 cm^{-1} attributed to ligand to metal charge transfer [22]. La(III) and UO_2(VI) and complexes are diamagnetic.

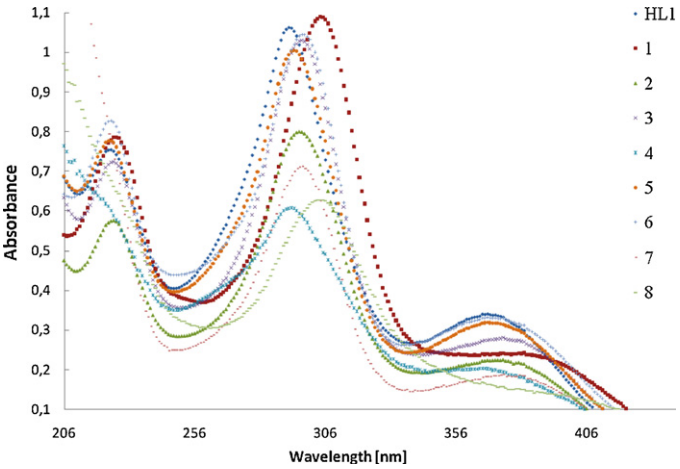

Fig. 2. UV–Vis absorption spectra (2.5×10^{-4} M) of binary complexes.

3.4. UV–Vis absorption spectra

The UV–Vis absorption spectra of the binary and ternary complexes (2.5×10^{-4} M) in ethanol–water mixture are shown in Figs. 2 and 3, respectively. The absorption spectrum of **HL_1** showed three absorption peak at 224, 292 and 366 nm and its molar absorptivities were in range of $(1.36–4.25) \times 10^3$ L mol^{-1} cm^{-1}; these peaks could be assigned to π–π^* and n–π^* transition within the organic ligand [24]. In all binary complexes the maximum absorption peaks had relatively high bathochromic shifts ($\Delta\lambda$ was in

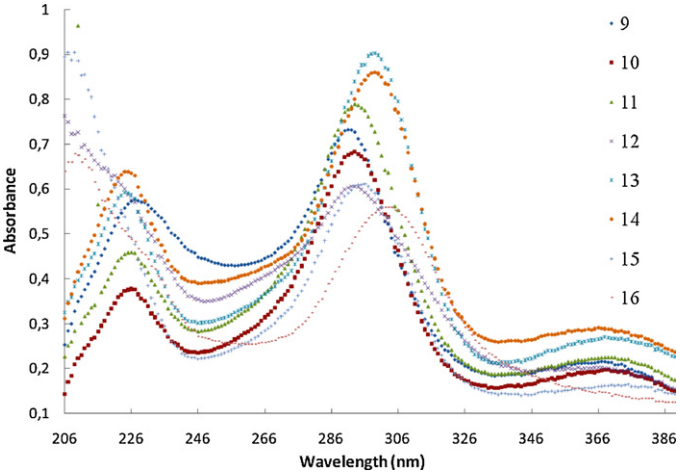

Fig. 3. UV–Vis absorption spectra (2.5×10^{-4} M) of ternary complexes.

the range of 1–16 nm) and their molar absorptivities were in the range of $(0.25–4.18) \times 10^3$ L mol^{-1} cm^{-1}, this can be attributed to the reaction of the metal ions with the ketonic oxygen and carboxylic oxygen in the conjugated system of the drug, which directly resulted in the changes of absorption spectra and bathochromic shifts of the maximum absorption peaks. Whereas in the case of ternary complexes new absorption peaks appeared in 340–352 nm and all the other absorption peaks are bathochromic shifted in the range of (1–11 nm) and their molar absorptivities were in the range of $(0.59–3.61) \times 10^3$ L mol^{-1} cm^{-1}, The shift of λ_{max} to higher values (bathochromic shift) and the decrease of the absorbance intensities in all of the mentioned complexes are indication to the complexation behavior towards metal ions. It was observed that in the case of lanthanides the energy of f–f transitions in the complexes is slightly reduced, this may be due to covalent interaction of 4f orbitals with vacant ligand orbitals or increased nuclear shielding of f-orbitals due to slight L–M electron transfer [25].

3.5. ^{1}H-NMR spectra

^{1}H-NMR spectra of uranyl and lanthanide complexes are recorded in DMSO-d_6. The ligand **HL_1** showed signals at 8.76 ppm due to NH_2 proton, which did not show any appreciable change in the complexes, confirming non-coordination of NH_2 moiety. The signals for the aliphatic piperazine and the methyl protons are practically unchanged since they lie far from the binding site of the ligand, also the cyclopropane protons remain practically unchanged as they were not involved in coordination. **HL_1** displayed a signal at 12.26 ppm characteristic of OH of carboxylic which was shifted downfield to about 1.24–1.64 ppm, indicative of coordination by the carboxylic group with deprotonation. In ternary complexes the carboxylic and amino protons are shifted downfield in comparison with alanine to about 0.52–1.39 ppm, indicating that the nitrogen and oxygen atoms are the probable coordination sites of alanine to the metal. A higherfield shift is observed for CH and methyl groups of DL-alanine on comparison with the spectra of the free amino acid; this may be due to formation of hydrogen bonding to the sulfoxide oxygen. In the complexes a broad peak is observed at 2.89 ppm, due to the presence of water molecules.

3.6. Thermal analysis

Thermal studies of the complexes have been done successfully by studying their simultaneous thermal analysis (TG/DTA). The decomposition data for the complexes is presented in Tables 4 and 5. The complexes are decomposed by losing water molecules and ligands in parts in different heating steps and ultimately in the final step metal oxide are found at high temperature.

The thermal decomposition of copper complexes are similar where the loss of hydrated water molecules are observed in the first step in case of ternary complex and second mass loss step in the case of binary complex between 50 and 250 °C. This process is strongly endothermic. A third mass loss step occurs in the range of 250–650 °C, the decomposition of the ligand is observed leaving CuO as a residue. This degradation process is accompanied by three successive exothermic peaks.

The same trend is observed in the case of the cobalt and nickel complexes, where the coordinated water is eliminated with an endothermic effect within the range of 50–400 °C in the first and second steps in case of cobalt and nickel binary complexes. While in case of ternary complexes the coordinated water is eliminated in the first step and connected with the exothermic processes within the temperature range of 50–200 °C. The third and fourth steps in cobalt and nickel binary chelates are accompanied with the decomposition of the ligand between 300 and 650 °C leaving NiO and CoO as a residue. This decomposition is connected with endothermic process. In the second and third steps in cobalt and nickel ternary complexes the decomposition of the ligand took place in the range of 200–750 °C leaving NiO and CoO as a residue. This decomposition is connected with exothermic process. In the last steps of decomposition, loss of the ligands took place leaving residual NiO and CoO between 200 and 750 °C. DTA shows three successive exothermic signals.

On the other hand the decomposition of manganese complexes exhibited three successive decomposition steps, the first step in the temperature range of 50–300 °C in which the complexes lose the coordinated water with an endothermic effect. The subsequent second and third steps (300–650 °C) correspond to the removal of the organic part of the ligand leaving metal oxide (MnO) as a residue. These steps are accompanied by two successive endo- and exothermic process.

TG of Cr(III)- and Fe(III) complexes showed liberation of hydrated and coordinated water and hydrated water molecules in the first and second steps with an endothermic effects. The third fourth and fifth steps are accounted for decomposition of ligands and loss of $0.5Cl_2$ leaving Cr_2O_3 and Fe_2O_3 residues, these three steps are accompanied by two endothermic and three exothermic DTA signals.

The TG of binary La(III) complex showed that the decomposition occurred in three closed steps within the temperature range of 50–650 °C. The first step in the range of 50–150 °C may be due to the liberation of hydrated water molecules accompanied with an endothermic effect. The second and third decomposition steps at 150–650 °C correspond to loss of coordinated water, liberation of NO_2 and $0.5O_2$ and decomposition of the ligand and formation of La_2O_3 as a final residue. These steps are connected with two endothermic effects. The thermal decomposition of ternary lanthanide complex showed similar behavior in four successive steps within the range of 50–630 °C, the first and second steps are responsible for removal of coordinated and hydrated water with an exothermic process. The third and fourth steps are accompanied with liberation of NO_2 and $0.5O_2$ and decomposition of ligands in the range of 240–630 °C. DTA represented an exothermic signal.

Uranyl binary and ternary complexes thermally decomposed in three and fifth decomposition steps, respectively. The first step in the range of 50–300 °C can be assigned to liberation of coordinated water with endothermic effects. The second till last mass loss steps in the range of 300–650 °C are accounted for the decomposition of both ligands molecules and formation of UO_2 as a final residue, this decomposition is followed by two endothermic and two exothermic signals.

3.7. Structures of the complexes

The structures of the binary Cu(II)- (**1**), Co(II)- (**2**), Ni(II)- (**3**), Mn(II)- (**4**), Cr(III)- (**5**), Fe(III)- (**6**), La(III)- (**7**), UO_2(VI)- (**8**) complexes with sparfloxacin (**HL_1**) and ternary Cu(II)- (**9**), Co(II)- (**10**), Ni(II)- (**11**), Mn(II)- (**12**), Cr(III)- (**13**), Fe(III)- (**14**), La(III)- (**15**), UO_2(VI)- (**16**) complexes with sparfloxacin (**HL_1**) and DL-alanine (**H_2L_2**) complexes are confirmed by the elemental analyses, IR, molar conductance, magnetic, UV–Vis, ESR, NMR and simultaneous thermal analysis. IR spectra revealed that **HL_1** drug behaves as a deprotonated bidentate ligand coordinated to the metal ions via pyridone oxygen and carboxylate oxygen. DL-Alanine is a uninegative bidentate ligand coordinated to the metal ions via the deprotonated carboxylate-O and amino-N. The molar conductance data, it is found that the complexes are non-electrolytes.

^{1}H-NMR spectra of **HL_1** displayed a signal at 12.26 ppm characteristic of OH of carboxylic, this signal shifted downfield by

Table 4
Thermal analysis data for binary complexes.

Complex	TG range, (°C)	DTG, (°C)	*n*	Mass loss	Total mass loss	Assignment	Metallic residue
				Found (calculated) (%)			
1	30–200	193	1	04.33 (04.07)		Loss of hydration water.	
	200–720	623	1	86.55 (86.93)	90.88 (91.00)	Decomposition of the $\mathbf{HL_1}$ ligand.	CuO
2	50–400	80,306	2	04.51 (04.10)		Loss of coordinated water.	
	400–650	446,570	2	87.05 (87.37)	91.56 (91.47)	Decomposition of the $\mathbf{HL_1}$ ligand.	CoO
3	50–300	78, 292	2	04.07 (04.10)		Loss of coordinated water.	
	300–600	409,465	2	87.50 (87.39)	91.57 (91.94)	Decomposition of the $\mathbf{HL_1}$ ligand.	NiO
4	50–280	215	1	04.61 (04.12)		Loss of coordinated water.	
	280–650	332,553	2	86.94 (87.78)	91.55 (91.90)	Decomposition of the $\mathbf{HL_1}$ ligand	MnO
5	50–240	90, 167	2	03.05 (03.97)		Loss of hydrated and coordinated water.	
	240–600	301, 89,580	3	79.67 (79.26)	82.72 (83.23)	Loss of $0.5Cl_2$ and decomposition of the $\mathbf{HL_1}$ ligand	Cr_2O_3
6	50–200	98	1	02.08 (01.98)		Loss of hydrated and coordinated water.	
	200–650	279, 502	2	80.00 (80.49)	82.08 (82.47)	Loss of $0.5Cl_2$ and decomposition of the $\mathbf{HL_1}$ ligand	Fe_2O_3
7	50–150	82	1	03.44 (03.47)		Loss of hydration water.	
	150–650	302,521	2	64.08 (65.14)	67.52 (68.61)	Loss of coordinated water, liberation of NO_2 and $0.5O_2$ and decomposition of the $\mathbf{HL_1}$ ligand.	La_2O_3
8	50–300	200	1	01.80 (01.68)		Loss of coordinated water.	UO_2
	300–650	273, 553	2	72.27 (73.10)	74.07 (47.78)	Decomposition of the $\mathbf{HL_1}$ ligand.	

n, number of decomposition steps.

the effect of complexation, In ternary complexes the carboxylic and amino protons are shifted downfield in comparison with alanine, indicating that the nitrogen and oxygen atoms are involved in the coordination. On the basis of the above observations and from the magnetic measurements, most of the complexes are six-coordinated with distorted octahedral geometry while Cu(II) complexes adopted square planar structure on the other hand U- and La-atoms have a pentagonal bipyramidal coordination sphere. The structures of the metal complexes can be given as shown below (Fig. 4).

3.8. Anti microbial studies

From a medical point of view, the discovery of new therapeutical targets and the development of new antibacterial, antiparasitical and antiviral drugs are urgently required, that is due to the emergence and alarming spread of bacterial, parasitical and viral strains that are resistant against the drugs used at present in clinics. Metal ions play a vital role in a vast number of widely different biological processes. The interaction of these ions with biologically active ligands, for example in drugs, is a subject

Table 5
Thermal analysis data for ternary complexes.

Complex	TG range, (°C)	DTG, (°C)	*n*	Mass loss	Total mass loss	Assignment	Metallic residue
				Found (calculated) (%)			
9	50–200	168	1	05.95 (06.21)		Loss of hydration water.	
	200–650	210, 306, 579	3	80.57 (80.06)	86.52 (86.27)	Decomposition of the $\mathbf{HL_1}$ and $\mathbf{H_2L_2}$ ligands.	CuO
10	50–200	80	1	06.40 (06.27)		Loss of coordinated water.	
	200–750	334, 561	2	80.40 (80.69)	86.80 (86.96)	Decomposition of the $\mathbf{HL_1}$ and $\mathbf{H_2L_2}$ ligands	CoO
11	50–200	70	1	06.22 (06.27)		Loss of coordinated water.	
	200–600	285, 322, 489	3	80.38 (80.72)	86.60 (86.99)	Decomposition of the $\mathbf{HL_1}$ and $\mathbf{H_2L_2}$ ligands	NiO
12	60–300	105	1	06.25 (06.31)		Loss of coordinated water.	
	300–600	323, 487, 530	2	81.11 (81.26)	87.36 (87.57)	Decomposition of the $\mathbf{HL_1}$ and $\mathbf{H_2L_2}$ ligands	MnO
13	50–300	103	1	05.43 (05.97)		Loss of hydration and coordinated water.	Cr_2O_3
	300–650	395, 503, 600	3	68.99 (68.82)	74.42 (74.79)	Loss of $0.5Cl_2$, decomposition of the $\mathbf{HL_1}$ and $\mathbf{H_2L_2}$ ligands	
14	50–200	80, 145	1	03.25 (02.97)		Loss of hydration and coordinated water.	
	200–600	240, 403, 587	3	70.17 (70.73) 73.42 (73.70)		Loss of $0.5Cl_2$, decomposition of the $\mathbf{HL_1}$ and $\mathbf{H_2L_2}$ ligands	Fe_2O_3
15	50–240	118, 208	2	05.11 (05.02)		Loss of hydrated and coordinated water.	
	240–630	397, 540	2	50.03 (49.41)	55.14 (54.43)	liberation of NO_2 and $0.5O_2$ and decomposition of the $\mathbf{HL_1}$ and $\mathbf{H_2L_2}$ ligands	La_2O_3
16	50–300	228	1	02.10 (02.35)		Loss of coordinated water.	UO_2
	300–600	280,365,480, 574	4	61.93 (62.38)	64.03 (64.73)	Decomposition of the $\mathbf{HL_1}$ and $\mathbf{H_2L_2}$ ligands	

n, number of decomposition steps.

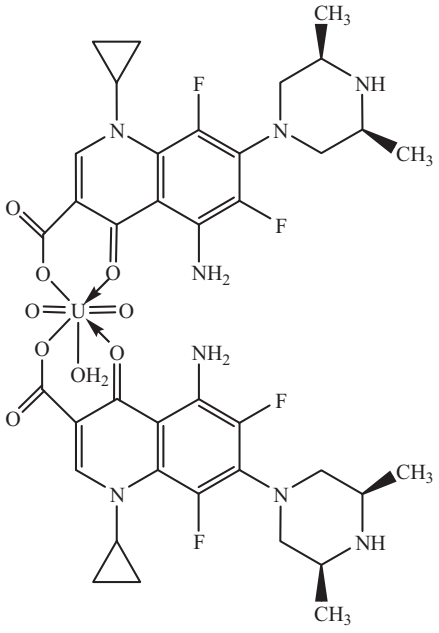

UO_2(VI) binary complex

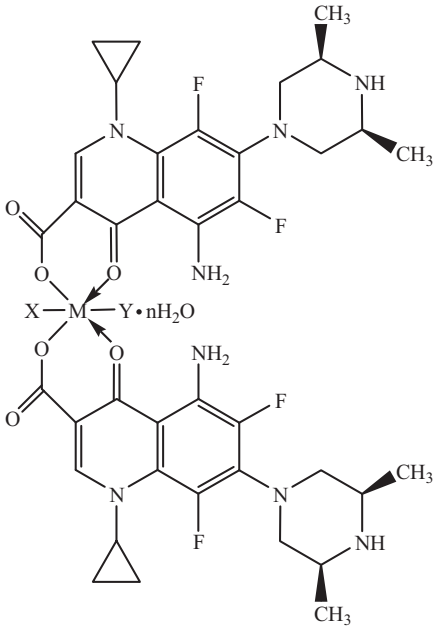

M = Cu(II), X = Y = 0, n = 2

M = Co(II),Ni(II), Mn(II), X = Y = H_2O, n = 0

M = Cr(III), Fe(III), X = Cl, Y = H_2O, n = 1

M = La(III), X = NO_3, Y = H_2O, n = 2

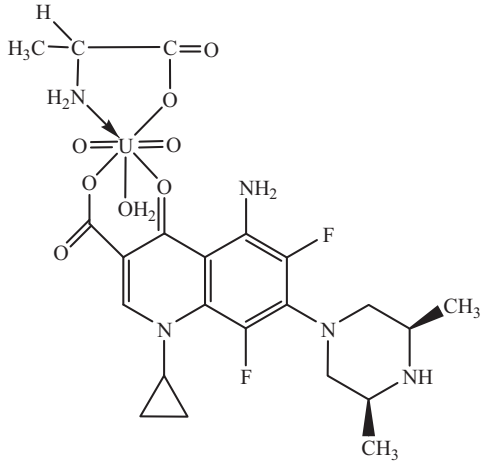

UO_2(VI) ternary complex

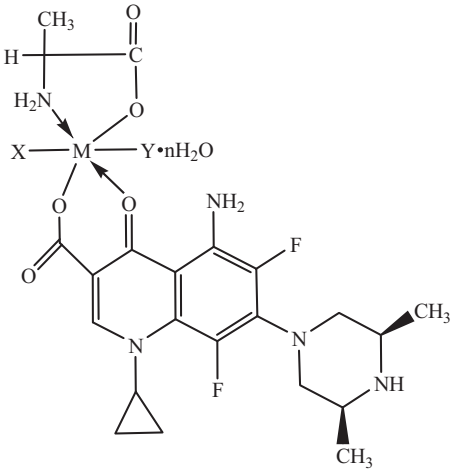

M = Cr(III), Fe(III), X = Cl, Y = H_2O, n = 1

M = Cu(II), Co(II), Ni(II), Mn(II), X = Y = H_2O, n = 0

M = La(III), X = NO_3, Y = H_2O, n = 1

Fig. 4. Proposed chemical structures of the metal complexes.

of considerable interest. Some of the biologically active compounds act via chelation [26], but for most of them is known about how metal binding influences their activity. Our target is to produce and evaluate some potential antimicrobial compounds without causing any side effects on the patients; therefore we have been interested in studying the complexing ability of biologically active ligands like sparfloxacin and discuss the coordination chemistry behavior of some metal ion and/or in presence of DL-alanine.

In evaluating the antimicrobial activity of the mentioned complexes we used more than one test organism in order to increase the chance of identify and observe the biological efficiency of the tested materials. The studies were carried out on, *S. aureus* (G^+), *E. coli* (G^-) species in bacteria and *A. flavus* and *C. Albicams* among fungi using assay plates disc method on appropriate nutrient medium. The results are included in Figs. 5 and 6, the inhibition zone diameters were measured after 48 h at 37 °C of incubation for all the mentioned complexes (Table 6). On comparing the biological activity of the sparfloxacin and its metal complexes with the standard (tetracycline, antibacterial) and (Amphotericin B, antifungal), the following results are obtained:

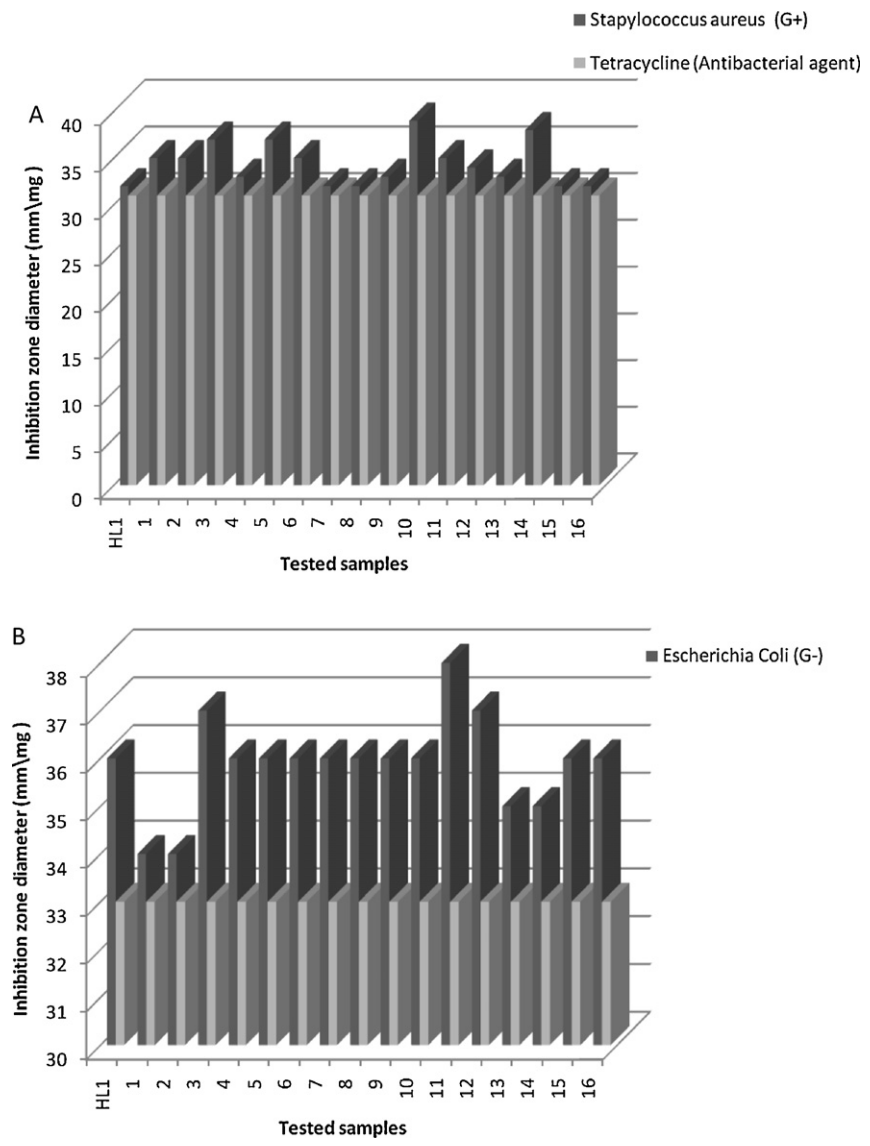

Fig. 5. Biological activity of $\mathbf{HL_1}$ and its complexes against (A, G^+), (B, G^-) bacteria.

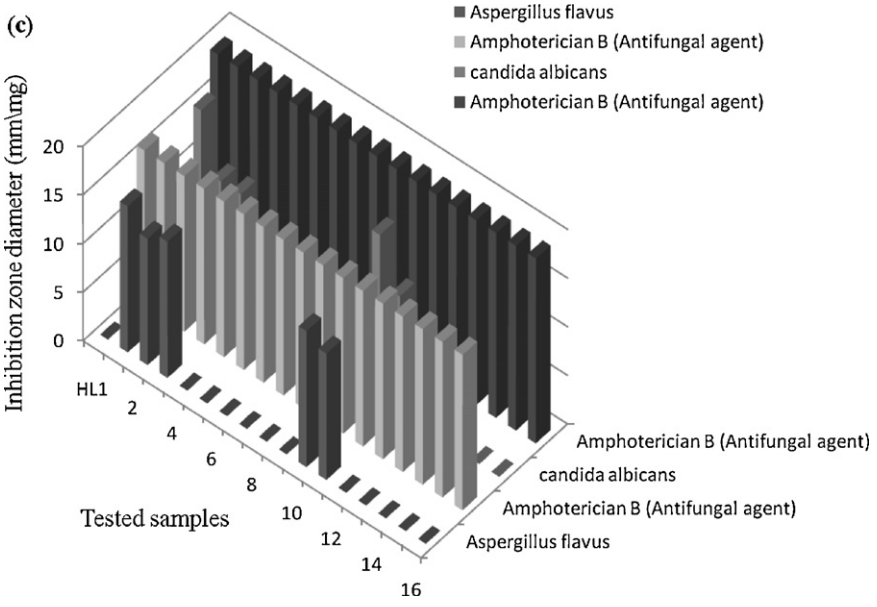

Fig. 6. Fungal activity of $\mathbf{HL_1}$ and its complexes against *Aspergillus flavus* and *Candida albicans* fungus.

Table 6
Antimicrobial activity of metal complexes and the standard effects of antibacterial and antifungal agents.

Diameter of zone of inhibition (mm)								
Complexes	*Stapylococcus aureus* (G^+)	Tetracycline (antibacterial agent)	*Escherichia coli* (G^-)	Tetracycline (antibacterial agent)	*Aspergillus flavus*	Amphoterician B (antifungal agent)	*Candida albicans*	Amphoterician B (antifungal agent)
Distilled water, chloroform, DMSO	0	0	0	0	0	0	0	0
HL_1	32	31	36	33	0	16	0	19
1	35	31	34	33	15	16	18	19
2	35	31	34	33	13	16	12	19
3	37	31	37	33	14	16	12	19
4	33	31	36	33	0	16	0	19
5	37	31	36	33	0	16	0	19
6	35	31	36	33	0	16	0	19
7	32	31	36	33	0	16	0	19
8	32	31	36	33	0	16	0	19
9	33	31	36	33	0	16	0	19
10	39	31	36	33	14	16	17	19
11	35	31	38	33	13	16	12	19
12	34	31	37	33	0	16	0	19
13	33	31	35	33	0	16	0	19
14	38	31	35	33	0	16	0	19
15	32	31	36	33	0	16	0	19
16	32	31	36	33	0	16	0	19

3.8.1. Staphylococcus aureus (G^+)

The free **HL_1** ligand showed higher antibacterial effect that the standard tetracycline, furthermore, the biological activity of binary and ternary complexes of Cu(II), Co(II), Ni(II), Mn(II), Cr(III), and Fe(III) complexes is higher than that of the free **HL_1** ligand and standard tetracycline. While, UO_2(VI) and La(III) binary and ternary complexes have the same biological activity of **HL_1** ligand and higher than that of tetracyclin. (Fig. 5), the biological activity of the complexes are found to follow the order **10 > 15 > 3 = 5 > 4 > 6 = 1 = 2 = 11 > 12 > 9 > HL_1 = 15 = 16 > 13 > standard tetracycline**.

3.8.2. Using Escherichia coli (G^-)

The biological activity of the **HL_1** ligand is found to be higher than that of the tetracycline standard, whereas binary [Mn(II), Cr(III), Fe(III), La(III) and UO_2 (VI)] and ternary [Cu(II), Co(II), La(III) and UO_2(VI)] complexes represented an equal activity to **HL_1** ligand, while binary Ni(II) and ternary Ni(II) and Mn(II) complexes showed a higher biological activity than both **HL_1** ligand and standard tetracycline. On the other hand binary [Cu(II) and Co(II)] and ternary [Cr(III) and Fe(III)] complexes represented less activity than **HL_1** but higher than standard tetracycline (Fig. 5). The order of activity can be arranged as follow **11 > 12 = 3 > HL_1 > 4 > 5 > 6 > 7 > 8 > 9 > 10 > 15 > 16 > 13 = 14 > 1 > 2> standard tetracycline**.

The significance of these results could be applied completely in the treatment of some diseases caused by *E. coli* like, Gastroenteritis, Septicaemia, Urinary tract infections and hospital required infections [27,28]. Many clinical research have been interested in finding new anti-tumours depends mainly on attacking Gram-negative bacteria [29–31], and since there are certain organisms difficult to attack as most of them are Gram-negative rods, therefore the complexes which showed higher biological activity against the Gram-negative strains may represent powerful attacking to the barrier function as mentioned by Brown [31] and Nikaido et al. [29]; therefore, the synthesis of these complexes might be recommended in order to establish a new branch of research dealing with the anti-tumour effect of many synthetic compounds as described by Hodnett et al. [31] and Hickman [32]. Thus we are claimed that these complexes may have a possible anti-tumour effect depending on the fact that, Gram-negative bacteria can be considered a quantitative microbiological method examine potent and useful drugs in both clinical and experimental tumour chemotherapy [33].

3.8.3. Using Aspergillus flavus and Candida albicans (Fungus)

HL_1 and most of binary and ternary complexes did not represent any fungal activity comparing to the standard Amphotericin B, nevertheless binary and ternary Co(II) and Ni(II) as well as ternary Mn(II) complexes showed some fungal activity, this activity is relatively less than the standard Amphotericin B (Fig. 6). The order of activity can be arranged as follow: standard Amphotericin B > **1 > 3 = 10 > 2 = 11** (in case of *A. flavus*) while in case of *C. albicans* the order can be as follows Amphotericin B > **10 > 2 = 3 = 11**.

By comparing the evaluation of the antimicrobial activity of these complexes with the previous published quinolones complexes, similar effects have been reported, very recently Sadeek et al. represented, that uranium, zirconium and yttrium complexes with sparfloxacin and gatifloxacin showed a good activity against Gram −ve and Gram +ve than drugs alone, while no antifungal activity is observed for both drugs and metal complexes [34], on the other hand Ni(II) and Ag(I) enoxacin complexes represented slight activity against Gram +ve and Gram −ve bacteria [35], while Cu–ciprofloxacin showed high standard antibacterial activity against Gram +ve and Gram −ve [36], the same effect is reported in the case of Fe–ciprofloxacin, where also no significant inhibition towards the growth of fungal strains are reported [37].

4. Conclusion

In this article, we describe the synthesis and characterization of binary and ternary complexes of sparfloxacin (**HL_1**) with DL-alanine (**H_2L_2**). Elemental analysis of C, H and N data obtained were in agreement with the predicted formula. Data of the infrared and ^{1}H-NMR spectroscopy represented that sparfloxacin acts as a bidentate deprotonated ligand bound to the metal through pyridone oxygen and carboxylate oxygen. DL-Alanine is a uninegative bidentate ligand coordinated to the metal ions via the deprotonated carboxylate-O and amino-N. All the complexes are six-coordinated with distorted octahedral geometry while Cu(II) complexes which have square planar structure from ESR parameters, magnetic and solid reflectance measurements. On the other hand uranyl and lanthanide complexes have a pentagonal bipyramidal coordina-

tion sphere. It has been observed that the metal complex have a high activity than ligand against same organisms under the identical experimental condition. The comparison of inhibition zone values for the newer metal complexes (Table 6) with another previous quinolones complexes reveals that the antimicrobial activity is quite high which could be an indication to generate useful information that contributes to the differentiation of new biomedical branches.

References

[1] (a) B.B. Lohray, V.B. Lohray, B.K. Srivastava, P. Kapadnis, P.P. Pandya, Bioorg. Med. Chem. 12 (2004) 4557–4564;
(b) D.E. King, R. Malone, S.H. Lilley, Am. Fam. Physician 61 (2000) 2741–2748;
(c) C.H. Gross, J.D. Parsons, T.H. Grossman, P.S. Charifson, S. Bellon, J. Jernee, M. Dwyer, S.P. Chambers, W. Markland, M. Botfield, S.A. Raybuck, Antimicrob. Agents Chemother. 47 (2003) 1037–1046;
(d) J.E.F. Reynolds, The Extra Pharmacopeia, 30th ed., The Pharmaceutical Press, London, 1993, pp. 145–147;
(f) M.V.N. de Souza, Mini-Rev. Med. Chem. 5 (2005) 1009–1017;
(g) G. Anquetin, J. Greiner, N. Mahmoud, M. Santillana-Hayat, R. Gozalbes, K. Farhati, F. Derouin, A. Aubry, E. Cambau, P. Vierling, Eur. J. Med. Chem. 41 (2006) 1478–1493.

[2] (a) D.T.W. Chu, P.B. Fernandes, in: B. Testa (Ed.), Advances in Drug Research, vol. 21, Academic Press, London, 1991, pp. 39–144;
(b) D.E. King, R. Malone, S.H. Lilley, Am. Fam. Physician 61 (2000) 2741;
(c) Sparfloxacin, in: J.K. Aronson (Ed.), Meyler's Side Effects of Drugs: The International Encyclopedia of Adverse Drug Reactions and Interactions, Elsevier, 2006, pp. 3172–3174.

[3] (a) I. Turel, Coord. Chem. Rev. 232 (2002) 27–47;
(b) K.C. Skyrianou, C.P. Raptopoulou, V. Psycharis, D.P. Kessissoglou, G. Psomas, Polyhedron 28 (2009) 3265–3271;
(c) M. Ruiz, L. Perelloï, J. Server-Carrioï, R. Ortiz, S. Garcıĭa-Granda, M.R. Diaz, E. Canto'n, J. Inorg. Biochem. 69 (1998) 231–239;
(d) B. Macias, M.V. Villa, M. Sastre, A. Castiñeiras, J. Borraïs, J. Pharm. Sci. 91 (2002) 2416–2423;
(e) Z.H. Chohan, C.T. Supuran, A. Scozzafava, J. Enzyme, Inhib. Med. Chem. 20 (2005) 303–307;
(f) Z.H. Chohan, H. Pervez, A. Rauf, C.T. Supuran, Met. Based Drugs 8 (2001) 263–267;
(g) M.P. Loïpez-Gresa, R. Ortiz, L. Perelloï, J. Latorre, M. Liu-Gonzaï lez, S. Garcıĭa-Granda, M. Peïrez-Priede, E. Cantoï n, J. Inorg. Biochem. 92 (2002) 65–74;
(h) J.R. Anacona, C. Toledo, Trans. Met. Chem. 26 (2001) 228;
(i) I. Turel, L. Golic, P. Bukovec, M. Gubina, J. Inorg. Biochem. 71 (1998) 53–60;
(j) I. Turel, I. Leban, N. Bukovec, J. Inorg. Biochem. 66 (1997) 241–245;
(k) F. Gao, P. Yang, J. Xie, H. Wang, J. Inorg. Biochem. 60 (1995) 61–67.

[4] S. Jain, N.K. Jain, K.S. Pitre, J. Pharm. Biomed. Anal. 29 (2002) 795–801;
(b) E.K. Efthimiadou, Y. Sanakis, C.P. Raptopoulou, A. Karaliota, N. Katsarosa, G. Psomasa, Bioorg. Med. Chem. Lett. 16 (2006) 3864–3867.

[5] (a) L.M.M. Vieira, M.V. de Almeida, H.A. de Abreu, H.A. Duarte, R.M. Grazul, A.P.S. Fontes, Inorg. Chim. Acta 362 (2009) 2060–2064;
(b) L.M.M. Vieira, M.V. de Almeida, M.C.S. Lourenço, F.A.F.M. Bezerra, A.P.S. Fontes, Eur. J. Med. Chem. 44 (2009) 4107–4111;
(c) M. Ruiz, R. Ortiz, L. Perelloï, S. Garcıĭa-Granda, M.R. Dıĭaz, Inorg. Chim. Acta 217 (1994) 149–154.

[6] H. Beraldo, D. Gambino, Mini-Rev. Med. Chem. 4 (2004) 31–39;
(b) J.R. Anacona, C. Toledo, Trans. Met. Chem. 26 (2001) 228–231;
(c) C. Chulvi, M.C. Muñoz, L. Perelloï, R. Ortiz, M.C. Muñoz, M.I. Arriortua, J. Via, K. Urtiaga, J.M. Amigoï, L.E. Ochando, J. Inorg. Biochem. 42 (1991) 133–138;
(d) M. Ruiz, R. Ortiz, L. Perelloï, A. Castiñeiras, M. Quiroïs, Inorg. Chim. Acta 211 (1993) 133–139.

[7] N. Sultana, M. Saeed, S. Gul, S. Shamim, J. Mol. Struct. 975 (2010) 285–291.

[8] (a) A.W. Bauer, W.M. Kirby, C. Sherris, M. Turck, Antibiotic susceptibility testing by a standardized single disk method, Am. J. Clin. Pathol. 45 (1966) 493–496;
(b) National Committee for Clinical Laboratory Standards. (2002). Reference Method for Broth Dilution Antifungal Susceptibility Testing of Conidium-Forming Filamentous Fungi: Proposed Standard M38-A. NCCLS, Wayne, PA, USA.

[9] M.A. Pfaller, L. Burmeister, M.A. Bartlett, M.G. Rinaldi, Multicenter evaluation of four methods of yeast inoculum preparation, J. Clin. Microbiol. 26 (1988) 1437–1441.

[10] J.A. Dean (Ed.), Lange's Handbook of Chemistry, 14th ed., McGraw-Hill, New York, 1992, Table 8.35.

[11] E. Santi, M.H. Torre, E. Kremer, S.B. Etcheverry, E.J. Baran, Vib. Spectrosc. 5 (1993) 285–293.

[12] E. Prestch, T. Clerc, J. Seibl, W. Simon, Tablas de Determinacion Estructural por Metodos Espectroscopicos, Springer-Verlag Iberica, Barcelona, 1998.

[13] N. Jimenez-Garrido, L. Perello, R. Ortiz, G. Alzuet, M. Gonzalez-Alvarez, E. Canton, M. Liu-Gonzalez, S. Garcia-Granda, M. Perez-Priede, J. Inorg. Biochem. 99 (2005) 677–689.

[14] (a) M.A. Zayed, F.A. Nour El-Dien, G.G. Mohamed, N.E.A. El-Gamel, Spectrochim. Acta 64A (2006) 216–232;
(b) M.A. Zayed, F.A. Nour El-Dien, G.G. Mohamed, N.E.A. El-Gamel, Spectrochim. Acta 60A (2004) 2843–2852;
(c) S. El-Khateeb, S. Abdel Fattah, S. Abdel Razeg, M. Tawakkol, Anal. Lett. 22 (1989) 101–115;
(d) W. Radecka-Paryzek, E. Luks, Monatsh. Chem. 126 (1995) 795–798;
(e) J. Costamagna, F. Carruso, M. Rossi, M. Campos, J. Canales, J. Ramirez, J. Coord. Chem. 54 (2001) 247–259;
(f) G.G. Mohamed, N.E.A. El-Gamel, Spectrochim. Acta 60A (2004) 3141–3151;
(g) G.G. Mohamed, N.E.A. El-Gamel, Vib. Spectrosc. 36 (2004) 97–104.

[15] (a) R. Wysokinïski, B. Morzyk-Ociepa, T. Głowiak, D. Michalska, J. Mol. Struct. 606 (2002) 241–251;
(b) F.R. Allen, O. Kennard, D.G. Watson, L. Brammer, A.G. Orpen, R. Taylor, J. Chem. Soc. Perkin Trans. 2 (1987) S1–S19;
(c) E.J. Baran, R.C. Mercader, F. Hueso-Ureña, M.N. Moreno-Carretero, M. Quiros-Olozabal, J.M. Salas-Peregrin, Polyhedron 15 (1996) 1717–1721;
(d) S. Lencioni, A. Pellerito, T. Fiore, A.M. Giuliani, L. Pellerito, M.T. Cambria, C. Mansueto, Appl. Organomet. Chem. 13 (1999) 145–157.

[16] Z. Ji, Y. Chen, X. Cheng, G. Chen, J. Chem. Crystallogr. 32 (2002) 141–145.

[17] N.E.A. El-Gamel, D. Gerlach, J. Coord. Chem. 61 (2008) 2246–2265.

[18] (a) G.M.R. Larin, J. Coord. Chem. 25 (1999) 804–810;
(b) S. Djebbar-Sid, O. Benali-Baitich, J.-P. Deloume, Polyhedron 16 (1997) 2175–2182.

[19] B.J. Hathaway, A.A.G. Tomlinson, Coord. Chem. Rev. 5 (1970) 1–43.

[20] S.-F. Tan, K.-P. Ang, Trans. Met. Chem. 13 (1998) 64–68.

[21] J. Manonmani, R. Thirumuruhan, M. Kandaswamy, V. Narayanan, S. Shanmuga, S. Raj, M.N. Ponnus Wamy, G. Shanmugan, H.K. Fun, Polyhedron 20 (2001) 3039–3048.

[22] F.A. Cotton, G. Wilkinson, C.A. Murillo, M. Bochmann, Advanced Inorganic Chemistry, 6th ed., Wiley, New York, 1999.

[23] A.B.P. Lever, Inorganic Electronic Spectroscopy, 1st ed., Elsevier, Amsterdam, 1968.

[24] C.-H. Song, H.W. Ryu, J.K. Park, T.-S. Ko, Bull. Kor. Chem. Soc. 20 (1999) 727–730.

[25] K.B. Gudasi, R.V. Shenoy, R.S. Vadavi, M.S. Patil, S.A. Patil, R.R. Hanchinal, S.A. Desai, H. Lohithaswa, Bioinorg. Chem. Appl. (2006) 1–8.

[26] A. Albert, Selective Toxicity. The Physico-Chemical Basis of Therapy, 6th ed., Chapman and Hall, London, 1979.

[27] E. Jawetz, J.L. Melnick, E.A. Adelberg, Review of Medical Microbiology, 16th ed., Lang Medical Publications, Los Anglos, CA, 1979.

[28] W.H. Hughes, H.C. Stewart, Concise Antibiotic Treatment, Butter Worth, London, 1970.

[29] H. Nikaido, T. Nakae, Adv. Microbiol. Phys. 20 (1979) 163–250.

[30] N.R.W. Brown, Resistance of *Pseudomonas aeruginosa*, vol. 71, John Wiley, 1975.

[31] E.M. Hodnett, A.W. Wu, F.A. French, Eur. J. Med. Chem. Chem. Ther. 13 (1987) 577–579.

[32] J.A. Hickman, Biochemie 60 (1987) 997.

[33] T. Inoue, Y. Yamashita, M. Nishihara, S. Sugiyama, Y. Sonoda, T. Kumabe, M. Yokoyama, T. Tominaga, Neuro-Oncology 11 (2009) 151–157.

[34] (a) S.A. Sadeek, W.H. El-Shwininy, J. Mol. Struct. 977 (2010) 243–253;
(b) S.A. Sadeek, W.H. El-Shwininy, J. Coord. Chem. 63 (2010) 3471–3482.

[35] Y. Cheng Liu, X.-J. Luo, C. Barta, H. Liang, J. Coord. Chem. 63 (2010) 3146–3154.

[36] Y. Wang, G.-W. Lina, J. Honga, L. Lia, Y.-M. Yanga, T. Lu, J. Coord. Chem. 63 (2010) 3662–3675.

[37] P.B. Pansuriya, M.N. Patel, J. Enzyme Inhib. Med. Chem. 23 (2008) 230–239.